Summary Of The Manufacture, Testing And Model Validation Of A Full-Scale Radiator For Fission Surface Power Applications

David Ellis[1], James Calder[2], John Siamidis[1]

[1]*NASA Glenn Research Center, 21000 Brookpark Rd., Cleveland, OH 44135*
[2]*Material innovations Inc., 15801 Chemical Lane, Huntington Beach, CA 92649*
Contact: David Ellis, 216-433-8736, David.L.Ellis@nasa.gov

Abstract. A full-scale radiator for a lunar fission surface power application was manufactured by Material innovations, Inc., for the NASA Glenn Research Center. The radiator was designed to reject 6 kW$_t$ with an inlet water temperature of 400 K and a water mass flow rate of 0.5 kg/s. While not flight hardware, the radiator incorporated many potential design features and manufacturing techniques for future flight hardware. The radiator was tested at NASA Glenn Research Center for heat rejection performance. The results showed that the radiator design was capable of rejecting over 6 kW$_t$ when operating at the design conditions. The actual performance of the radiator as a function of operational manifolds, inlet water temperature and facility sink temperature was compared to the predictive model developed by NASA Glenn Research Center. The results showed excellent agreement with the model with the actual average face sheet temperature being within $\pm$1% of the predicted value. The results will be used in the design and production of NASA's next generation fission power heat rejection systems. The NASA Glenn Research Center's Technology Demonstration Unit will be the first project to take advantage of the newly developed manufacturing techniques and analytical models.

Keywords: Radiator, heat pipe, modeling, performance

INTRODUCTION

Future lunar, Mars and other missions will require substantial electrical power. For example, current concepts for potential lunar outposts indicate the need for 30 to 80 kW$_e$[1]. One possible source of this electrical power, shown in Figure 1, is a fission surface power system[1]. Such a system would consist of a small nuclear reactor, Stirling power conversion units, and a waste heat rejection system. The heat rejection system would consist of pumps, accumulators, feed lines, manifolds, and heat pipe radiator panels mounted in a deployable frame. The Second Generation Radiator Demonstration Unit (RDU) project examines the integration and manufacture of the radiator panel, heat pipes and manifolds into a basic radiator unit assembly. The radiator assembly underwent extensive testing at the National Aeronautics and Space Administration (NASA) Glenn Research Center (GRC) in Vacuum Facility #6 (VF #6). The data generated was subsequently compared to a Thermal Desktop model of the radiator unit and the test facility to validate the model and demonstrate the ability to successfully model the radiator. This paper presents information on the manufacturing of the Second Generation RDU, selected test results under a wide variety of operating conditions, and the comparison of the test results to the model predictions.

Based upon current understanding of the fission surface power system that would be used for a lunar outpost, the average inlet water temperature would be 400 K, the water mass flow rate would be 0.5 kg/s, and the nominal sink temperature would be 250 K. With twenty panels, each radiator unit will need to reject an average of six kilowatts of thermal energy. The Second Generation RDU utilized prototypic design, materials of construction, production techniques, and size of components based upon lunar outpost power system requirements. Other missions may have different surface power requirements, but they are anticipated to have similar operating conditions and size

requirements. Considerations were given to overall heat transfer design, freeze-thaw cycling, thermal expansion mismatch, weight minimization, and thermal and gravity induced stresses. Lunar operational considerations were addressed by providing two independent, redundant manifolds to interface to the heat pipes. The Second Generation RDU and its structural frame are shown in Figure 2. Figure 2 also shows the frame used to suspend the radiator unit during testing. A portion of VF #6 including the cold wall used to chill the chamber can be seen in the background.

The Second Generation RDU incorporates several new technologies into its design that are candidates for future fission surface power applications. It uses titanium/water heat pipes at moderate temperatures between 370 K and 430 K. It utilizes high conductivity graphite fibers in a polymer matrix for the face sheets. It uses water for the heat transfer media and titanium in the manifolds. It is designed to operate after being frozen in transit with particular emphasis on minimizing thermal expansion mismatch and formation of ice that ruptures components. While some of these technologies have been used in the past, the Second Generation RDU is the first known application where all of the technologies are integrated and tested together which makes it unique. The results will feed directly into the follow-on Technology Demonstration Unit which will incorporate a representative heat rejection system with six radiators with a power conversion unit and simulated reactor heat source.

Production of the unit began in 2008. Following delivery of the radiator in March, 2009, integration and full-scale testing was initiated at GRC. After testing was completed the data was compared to the results predicted by a model developed at NASA GRC.
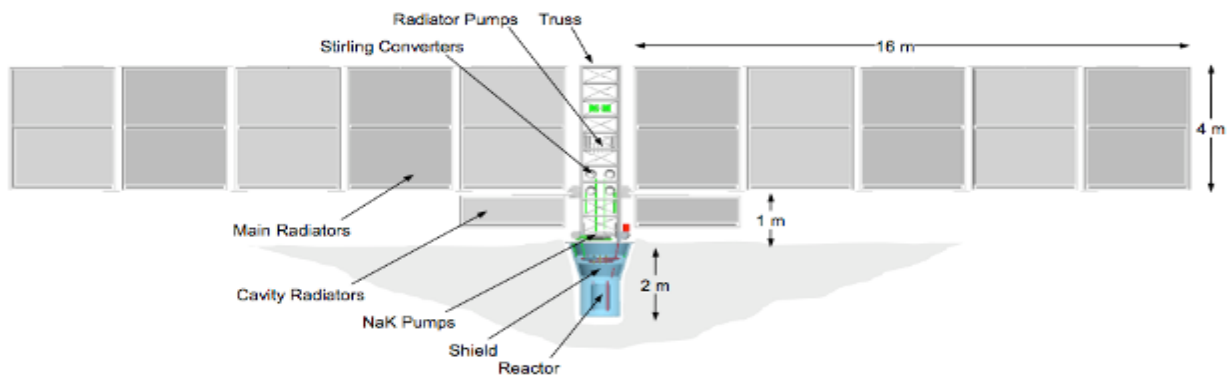
FIGURE 1. Fission Surface Power Concept System

The Second Generation RDU was designed and built by Material Innovations Inc. (MII) of Huntington Beach, CA for NASA GRC[2]. The design consists of two manifolds made from CP (Commercially Pure) Grade 2 titanium; sixteen CP Grade 2 titanium-water heat pipes, POCO HTC Foam® (aka POCO) graphite foam saddles to connect the heat pipes to the face sheets, and multiple K13D2U grade graphite fiber - EX1522 cyanate ester polymer matrix face sheets for the heat rejecting surface. Once assembled, the Second Generation RDU was approximately 2.0 m tall by 2.7 m wide (79 inches x 106 inches). The edges of the panel were closed out with pitch-based graphite/epoxy, glass fiber/epoxy, and compression molded graphite/epoxy fittings. The total length of the heat pipes was 1.97 m (77.6 inches) excluding the fill tube on the end of the condenser section. To provide representative optical properties for a lunar radiator, the face sheets were coated with Lord Aeroglaze® A276.

Mechanical modeling of the complete radiator assembly was completed by MII to correctly address geometric constraints, component integration, and manufacturing tool design. Figure 3 illustrates the final design assembly. Note that the front set of face sheets are removed in the figure for viewing the interior details.

FIGURE 2. Second Generation RDU Suspended In Vacuum Facility #6

MANUFACTURE OF THE SECOND GENERATION RDU
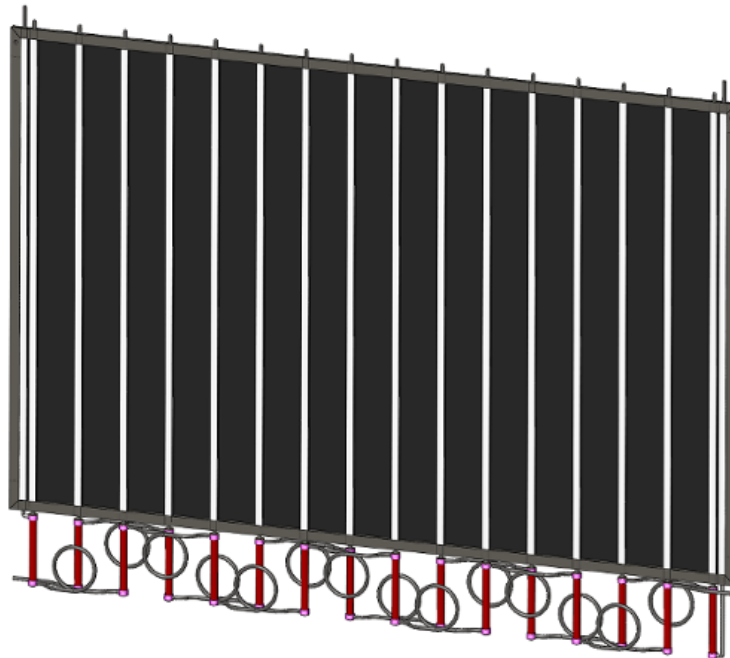
FIGURE 3. Second Generation RDU With Front Face Sheet Panel Sets Removed

The primary components shown include the vertical heat pipes with heat exchange manifolds around the evaporators at the bottom, two independent loops for the heated fluid flow, a closeout frame, the rear face sheets shown in black, and the graphite foam saddles shown as the vertical white elements.

Unique to this radiator was the plumbing design of the heated fluid passages. The coils shown in Figure 4 allowed for strain compliance to minimize the thermally induced stresses in the composite structures. These coils acted as reverse Bourdon Tubes in that they contract from connection to connection when the unit is pressurized and heated. This contraction minimizes the stresses that arise from the negative CTE of the composite structure.

Bending and welding of the manifold and heat exchanger assembly was based on the solid modeling shown above. Subcontractor Thermacore Inc of Lancaster, PA provided the design and delivery of the individual heat pipe elements and assemble the manifolds by welding. The connection tubes shown are 19 mm (0.75") diameter with 0.89 mm (0.035") thick walls that were formed with 75 mm (3 inch) radius loops. This was the minimum radius that could be produced with this diameter tube. Computational Fluid Dynamics (CFD) analysis was used to determine the tube diameter and to assure for a very low pressure drop along the length of this fluid circuit. In consideration for packaging, the distance between two connection circuits at the loops was minimized to 6.03 inch. The inlet and outlet cups were designed to simplify the bends in the connection tubes. The outlet cup also included an extra tab "leg" to minimize any torsion twisting incurred by the heat exchange manifold assembly during operation. An alignment bar attached to the ends was made from a CTE matching K13D graphite epoxy to assure for no mismatch stresses relative to the other graphite structures.
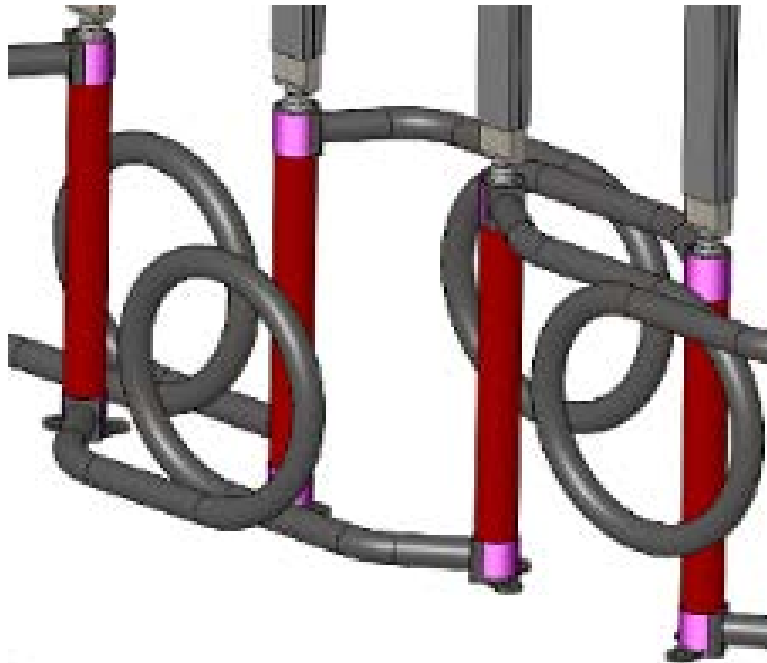
FIGURE 4. Detail View Of Second Generation RDU Showing Plumbing And Structural Elements

Tooling Design and Second Generation RDU Manufacture

The solid modeling of the Second Generation RDU also allowed for the design and easy manufacture of a wide variety of fixtures and components for assembly such as those shown in Figure 5, The welding fixture shown in Figure 5a held all of the components in place during fitting and welding of the heat pipes and manifolds. The final assembly tooling shown in Figure 5b held the pieces in the proper position, allowed fit checking before assembly, and applied the required pressure to properly bond the saddles and face sheets to the heat pipes. It also allowed access to the interior of the panel during manufacture to embed sensors. Throughout manufacturing and assembly all parts and joints underwent extensive inspection and quality control testing. The modular design allowed for the easy removal of parts that failed quality control and rework of joints that did not pass inspection.

MII transferred the solid designs to Computer Numerically Controlled (CNC) waterjet cutters and other suitable equipment to make the components of the manifolds and fixturing. The use of high precision components and

fixtures allowed for easy fitment check and assembly by Thermacore. The assembly sequence was carefully controlled to minimize residual stresses and deformations. Following assembly of the two manifolds and integration of the heat pipes, the assemblies were returned to MII for the addition of the saddles, face sheets and sensors.

The close-out frame "C-channel" was made of K13D/Epoxy for the horizontal direction and Glass/Epoxy for the vertical direction. The horizontal and vertical C-channel final layup tools were machined from 3.0 m (10 feet) and 2.1 m (7 feet) lengths of channel, respectively. Saddle production resulted in the output of 25 cm (10 inch) long pieces of foam saddle for Second Generation RDU assembly. Careful attention was given to machining precision, maintaining of open cell structure, and orientation of the cut. On the latter, it is critical to maintain orientation because the foam is highly anisotropic. The high thermal conductivity direction had to be maintained in the direction of the heat flow from the heat pipe to the face sheet.
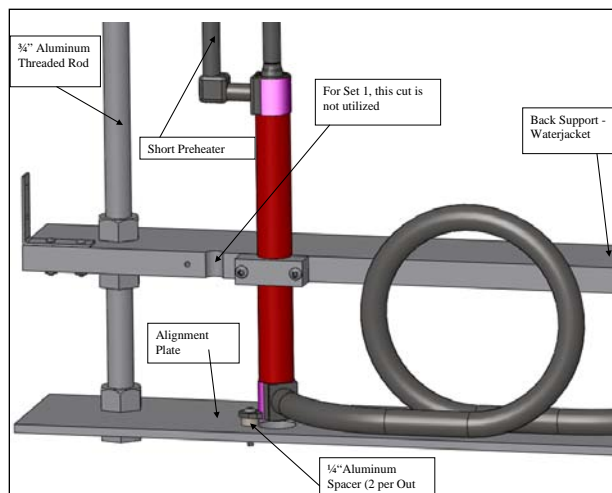
(a) Detail Of Welding Fixture Showing Manifold Ready For Welding
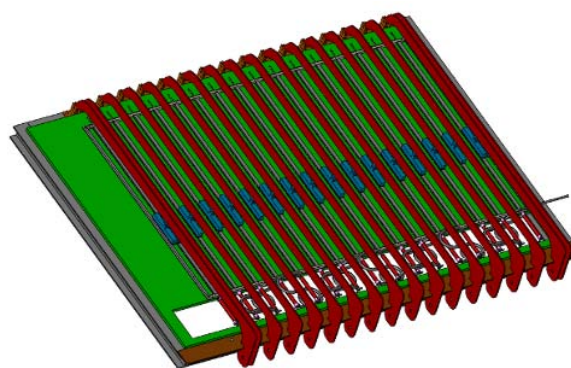
(b) Final Assembly Tooling

FIGURE 5. Examples Of Second Generation RDU Assembly Fixtures

To begin production the horizontal C-channel close-out frames were slid over the heat pipe structure and secured at the top and bottom of the heat pipe condenser section where the face sheets would be. This starting point in manufacturing provided the proper alignment for each heat pipe. The alignment staged the balance of manufacturing activity to bond together the saddle and face sheet structures. The horizontal close outs were bonded in place with internal compression molded structural inserts that tie the channels to the heat pipe condenser ends.

Saddles were prepared with a proprietary thermally conductive adhesive mixture and attached to the heat pipe evaporators. The heat pipe was sandwiched between two saddle halves. A predetermined load was applied thereafter to assure a good bond between the saddle and the heat pipe.

Eighteen strips of 0.3 m x 2.7 m (1 foot x 9 feet) face sheets were fabricated from K13D2U/ EX1522 prepreg tapes. The ply layup was determined through analysis and testing. The layup was biased for directional heat transport. All face sheets were made from a 6-ply laminate (0°/+11°/-11°/-11°/+11°/0°) with a total thickness of approximately 1 mm (0.041 inch). Final consolidation was carried out in an autoclave. Seven strips were required to complete each side of the Second Generation RDU. Twelve strips of K13D20U/EX1522 laminate 0.25 m x 2.7 m (10" x 105.6") in size were cut to make the majority of the face sheets. Two other sheets 2.7 m long were cut and fitted to width during final consolidation of the Second Generation RDU to cover the small remaining gap at the top of the radiator panel. Face sheet attachment was initiated after saddle installation was completed.

Figure 6 illustrates the attachment of internal resistance temperature detectors (RTDs) prior to joining the face sheet structure. These sensors were imbedded to measure temperature gradients within the Second Generation RDU structure during testing and evaluation at NASA GRC.

Spade Bros. Inc. was contracted to paint the Second Generation RDU panel. The subcontractor developed the required methods for applying the Lord Aeroglaze A276 coating to obtain a uniform coating with a mirror smooth finish. Commercial car painting equipment was used for the coating application.

FIGURE 6. Internal RTDs

An aluminum support frame with detachable wheels allowed easy movement of the Second Generation RDU. The base also allowed the frame to stand without additional support. The Second Generation RDU panel was suspended by braided stainless steel wires at the corners. Additional catch wires were attached at the top and sides. The frame without the wheels was also used at NASA GRC to suspend the Second Generation RDU in the vacuum facility (Figure 2). Delivery of the Second Generation RDU was made to NASA GRC in March 2009. MII provided installation support and technical support during the test period.

PERFORMANCE TESTING OF THE SECOND GENERATION RDU

Experimental Procedure

The Second Generation RDU was instrumented to provide the required performance information about the face sheets, POCO graphite foam saddles, heat pipes, manifolds and water. The face sheet temperatures were measured using Type T thermocouples. The water temperatures were measured using 1/10 DIN (Band 5) single element RTDs. The water volume flow rate for each manifold was measured using a Khrone Optiflux 5100 flow meter with IC 300 readout. Class B micro-RTDs were embedded within the panel on heat pipes 7 and 9 to provide internal panel temperature data.

Two hundred two channels were recorded using a custom data acquisition (DAQ) system running LabView. Analog to digital conversion was accomplished using a National Instruments' SCX-1600 DAQ module in an SCXI-1001 chassis. Seven SCXI-1102 32 channel thermocouple and one SCXI-1581 RTD current excitation modules were used to convert the thermocouple and RTD voltages into a digital temperature signal. End-to-end calibrations were done for all of the water RTDs and a representative subsample of the thermocouples and micro-RTDs before and after testing. The water flow meters were also calibrated before and after testing.

Hot water was supplied by a custom-designed 40 kW water heater manufactured by Heat Exchange And Transfer, Inc. Deionized water with a resistivity greater than 200 kΩ-cm was used for the heat transfer fluid. The water was heated and supplied by the water heater to the Second Generation RDU manifolds through stainless steel pipes.

VF #6 is a cylindrical vacuum chamber approximately 21.3 m (69 feet) long that has a 7.0 m (23 feet) inner diameter. The chamber includes a full axial-length liquid nitrogen cold wall with three independently controlled zones that can be chilled to a surface temperature of about 80 K. The Second Generation RDU was mounted in the middle of the chamber corresponding to the central cold wall zone. The cold wall extends 300° around the chamber with the bottom 60° and ends not being covered by the cold wall. The chamber was operated at a pressure between 0.7 mPa and 1 mPa during testing to provide the lunar-like vacuum environment and effectively eliminate convective heat transfer.

Four independent variables were identified for performance testing: operating manifold(s), inlet water temperature, water flow per manifold, and sink temperature. Inlet water temperature and water flow were continuously variable over the range of interest. Because of the nature of the manifolds, they were either on or off. Likewise, the cold wall was either on or off, so there were only two sink temperatures available. A Design of Experiment (DOE) was created to determine the heat dissipated as a function of the independent variables. Water flow was varied from 0.05 to 0.5 kg/s. The inlet water temperature was varied from 370 K to 430 K. Test points were repeated to ensure that good statistics could be generated for each test condition as well as to aid in curve fitting and model validation during the post-test data analysis.

The heat rejected by the Second Generation RDU was independently measured simultaneously by two methods. Details of the methods are discussed in Reference 3. The first method relies upon the decrease in enthalpy as heat is extracted from the water and rejected through the radiator. The heat rejected is calculated from the equation

$$Q = \dot{m}\left[h\left(T_{Inlet}, P_{Inlet}\right) - h\left(T_{Outlet}, P_{Outlet}\right)\right] \tag{1}$$

The second method used the average temperature of the face sheets and sink to calculate the heat rejected by radiation using the Stefan-Boltzmann equation

$$Q = A\sigma\varepsilon\left(T_{Panel}^4 - T_{Sink}^4\right) \tag{2}$$

Discrepancies in the heat rejection were noted, so a third method based upon the fin efficiency model work of Gilmore[4] and Chang[5] was utilized to evaluate the water temperature decrease required to match the radiation model heat rejections. The equation used was

$$Q = A\varepsilon\eta_e\sigma\left(T_B^4 - T_{Sink}^4\right) \tag{3}$$

Chang numerically solved the full differential equation for the fin efficiency to develop the equations

$$\begin{aligned}
\eta_e &= \left(1 - 1.125\varsigma + 4.60\varsigma^2\right)\left(1 - \theta^4\right) \quad 0.01 \leq \varsigma \leq 0.2 \\
&= \left(-0.405\log\varsigma + 0.532\right)\left(1 - \theta^4\right) \quad 0.2 \leq \varsigma \leq 2.0
\end{aligned} \tag{4}$$

Here ς and θ are defined by the equations

$$\varsigma = \frac{\sigma L^2 T_B^2 \left(\varepsilon_1 + \varepsilon_2\right)}{kt} \tag{5}$$

$$\theta = \frac{T_S}{T_B} \tag{6}$$

Using these equations and iterating to calculate an outlet water temperature allowed for the calculation of the required water temperature drop as well as the power.

Results And Discussion

The performance of the Second Generation RDU was defined by the heat that it could reject for a given inlet water temperature and water flow rate. The heat rejection as measured by the temperature difference of the water across the manifold (Equation 1) is shown in Figures 7, and the heat rejection based on thermal radiation calculated from the face sheet temperatures and the Stefan-Boltzmann Equation (Equation 2) is shown in Figure 8. The radiator performance is presented for both the cold wall off and on conditions.

In these figures, both manifolds are operational. Operating either manifold 1 or 2 alone produce similar shaped graphs. For brevity, these plots are not shown here. More complete information will be presented in the Second

Generation RDU Final Test Report[6]. As expected, the major difference with one manifold operating was a lower total heat rejection. At 400 K and a water mass flow rate of 0.25 kg/s per manifold (0.5 kg/s total for both manifolds operating), the average heat rejection for a single manifold operating was 73% of the two manifold operating. The heat rejection for the single manifold operation exceeds 50% of the dual manifold operation because the fin length and the area of the radiator associated with each manifold increases when the second manifold is turned off. This allows the operational manifold to radiate more heat.

This result has significant ramifications for lunar operations in that it demonstrates an ability to reject most of the reactor heat if one manifold is lost. That means that the electrical power available to a lunar outpost will remain high. The amount of heat can be increased further by increasing the inlet water temperature. An increase to 430 K results in the total heat rejected by one manifold reaching 95% that of two manifolds operating at 400 K. While material and equipment limitations will place a restriction on how high the water temperature can be raised, there is at least a reasonable path for retaining most of the power capability for the fission surface power system in the event a cooling loop is lost.

The Second Generation RDU heat rejection performance as a function of water mass flow rate through the manifolds was also examined. Figure 9 shows the heat rejected based upon the Stefan-Boltzmann Equation (Equation 2) for an inlet water temperature of 400 K. There is a distinct drop-off in the heat rejected at the lowest water mass flow rates. The heat transfer coefficient decreases as the water flow rate decreases, so the amount of heat that can be transferred from the water to the heat pipe decreases. Low flow rates may also promote laminar rather than turbulent flow which exacerbates the problem. The difference in heat rejection between moderate (0.25, 0.32 kg/s) and full (0.5 kg/s) water flows is relatively small.

The ability to reject over 6 kW_t at total water mass flow rates below even 0.2 kg/s when the cold wall is operating indicates that the fission surface power system may be capable of operating at a much lower water mass flow rate. The lower water mass flow rate would have to be traded against the water temperature decrease and heat rejection to optimize the heat rejection system, so it is not clear how much the water mass flow rate can be decreased and still meet the total heat dissipation requirement of the system. One implication of a lower water mass flow rate on the system is that the pump mass and power may be reduced. This would reduce both the total mass of the heat rejection system and the parasitic power required to run the heat rejection system. Both of these would be desirable for future fission surface power systems.

Even if a reduction in water mass flow rate is not implemented, the results show that some loss of flow can be tolerated. This means minor degradation of the pump and the heat transfer loops during operation of the power system will not have any real impact upon the ability of the heat rejection system to perform adequately. This will improve safety and mitigate risk in the heat rejection system.

(a) Cold Wall Off   (b) Cold Wall On
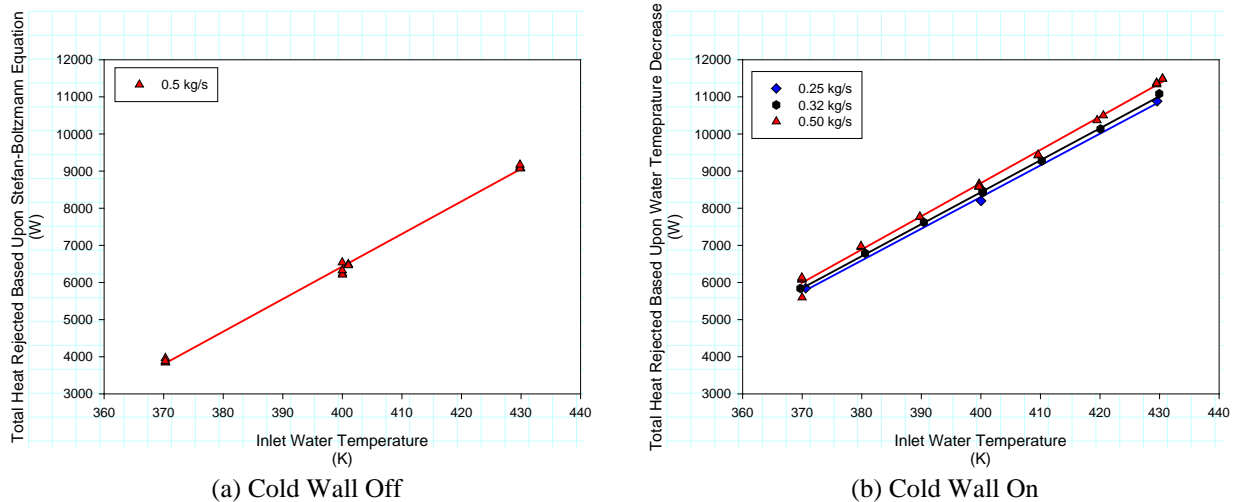
FIGURE 7. Heat Rejection Based Upon Water Temperature Decrease

(a) Cold Wall Off

(b) Cold Wall On
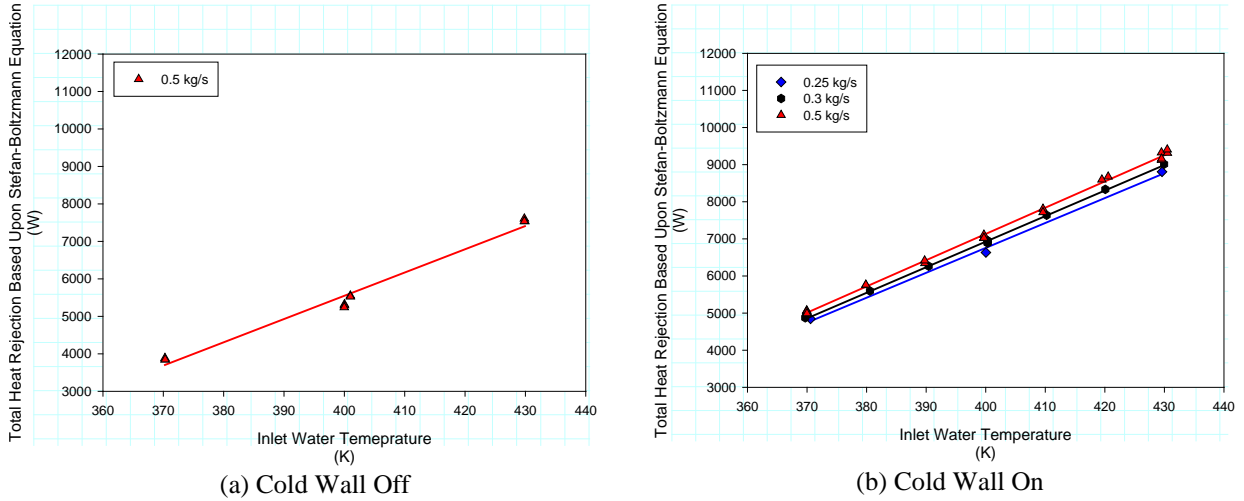
FIGURE 8. Heat Rejection Based Upon Average Face Sheet Temperature And Stefan-Boltzmann Equation
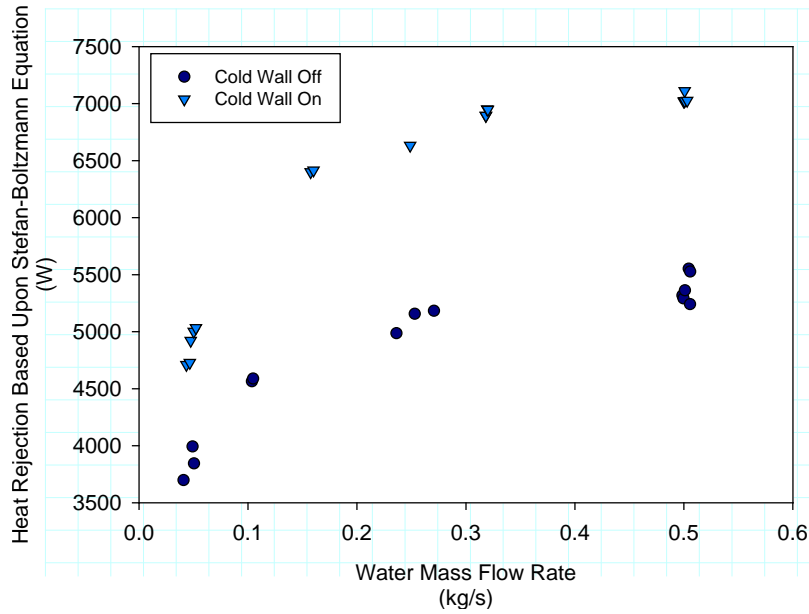
FIGURE 9. Heat Rejection With 400 K Inlet Water Temperature As A Function Of Water Mass Flow Rate

The difference between the heat rejection calculation based upon using the Stefan-Boltzmann Equation (Equation 2) and the calculation based upon the fluid heat change (Equation 1) is substantial. The heat rejection calculated from the manifold water temperature decrease is about 23% greater on average than that calculated from the Stefan-Boltzmann equation at all operating conditions. The analysis also showed that the difference is systematic rather than random since there is a strong linear correlation between the two heat rejection values. Sources of the disparity were investigated to determine possible causes.

Measurement error analysis was conducted by Integrated Sciences Group of Bakersfield, CA to determine how much the errors in the measuring devices could contribute to the difference in the powers calculated. A full analysis was done at 400 K and full flow (0.5 kg/s) with the cold wall on and both manifolds operating. Both the fluid heat loss and the radiation heat loss were analyzed. The results indicated that the total measurement error for the fluid heat loss was ±656 W or ±7.6% of the average measured value while the measurement error for the radiation heat loss was ±379 W or ±5.4% of the average measured value. In both cases, the temperature measurement error accounted for 95% of more of the total measurement error. Water mass flow measurements and other contributors

had very minimal effects. Based upon these results, a difference of 13% at most can be explained by measurement error. The difference at this condition is 18%. Therefore, measurement error alone cannot explain the difference between the two heat dissipation values even if the maximum measurement error is assumed.

Test results showed that the fin root temperatures were consistent and repeatable for both heat pipe sets. Calculations of the heat rejection based upon the methods of Gilmore and Chang (Equation 3) were compared with calculation of the heat rejection from the other two methods. The fin efficiency heat rejection values were very close to the values calculated from the average face sheet temperature and the Stefan-Boltzmann equation (Equation 2). When the outlet water temperatures from the fin efficiency model were compare to the measured outlet water temperatures, the differences were between 0.5k and 2 K for a water mass .flow rate of 0.5 kg/s. This highlights how much effect small changes in the change in water temperature can have on the calculated heat rejections. It also indicates that these measur~~ru~~ements are a likely cause of the observed differences.

The model also allows the calculation of the hat rejection at any sink temperature within the design space. Using a sink temperature of 250 K, the nominal full sun lunar heat sink temperature, the radiator is capable of rejecting 6,276 W at a water mass flow rate of 0.5 kg/s and an inlet water temperature of 400 K. This is 4.6% more than the nominal requirements, so Second Generation RDU was deemed to be successful.

To summarize the heat rejection performance with both manifolds operating, the Second Generation RDU had a wide range of heat rejections for the sink temperature, water flow rate and inlet water temperature tested. Using the values calculated from the Stefan-Boltzmann Equation, for the nominal flow condition of 0.5 kg/s total, the heat dissipated ranged from 3,350 W with an inlet water temperature of 370 K and the cold wall off to 9,270 W with an inlet water temperature of 430 K and the cold wall on. At the nominal inlet temperature of 400 K, with the cold wall on, the heat rejected based upon the Stefan-Boltzmann Equation ranged from 4880 W at a total water flow rate of 0.05 kg/s to 7040 W at a total water flow rate of 0.5 kg/s. Turning the cold wall off lowered the heat dissipated from 7040 W to 5386 W at a 400 K inlet water temperature and 0.5 kg/s water flow rate based upon the Stefan-Boltzmann Equation.

SECOND GENERATION RDU MODEL VALIDATION

Thermal Desktop from C&R Technologies was used to model the Second Generation RDU and VF #6. Thermal Desktop is a CAD-based modeling program, so design drawings could be imported into the program and used directly. It was necessary to model the internal details of the Second Generation RDU to understand the heat flow path and determine the anticipated temperature drops within the panel. Figure 10 shows the models used for the Second Generation RDU. Figure 11 shows the model used for Vacuum Facility #6. The model contains all major chamber features. The end caps and the bottom 60° of the chamber are uncooled and are modeled as such. The figure also shows the position of the Second Generation RDU within the VF #6 chamber during testing.

(a) Overview of Second Generation RDU Model

(b) Detail Of Second Generation RDU Internal Parts
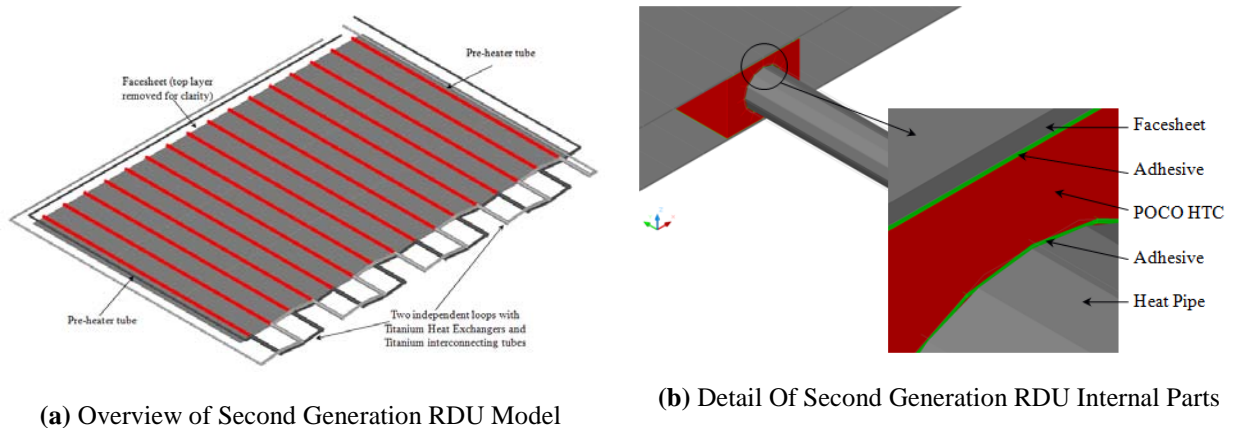
FIGURE 10. Second Generation RDU Thermal Desktop Model

Thermophysical properties for the Second Generation RDU were supplied by MII. The face sheet optical properties (emissivity and absorptivity) were measured at NASA GRC before and after testing and remained constant. The values for the heat pipes and manifolds are for titanium and are taken from a standard database used by NASA that was compiled by NASA Engineering and Safety Center[7]. The material values used in the model are presented in Table 1. The as-built masses of the Second Generation RDU were supplied by MII and were also incorporated into the Thermal Desktop model.
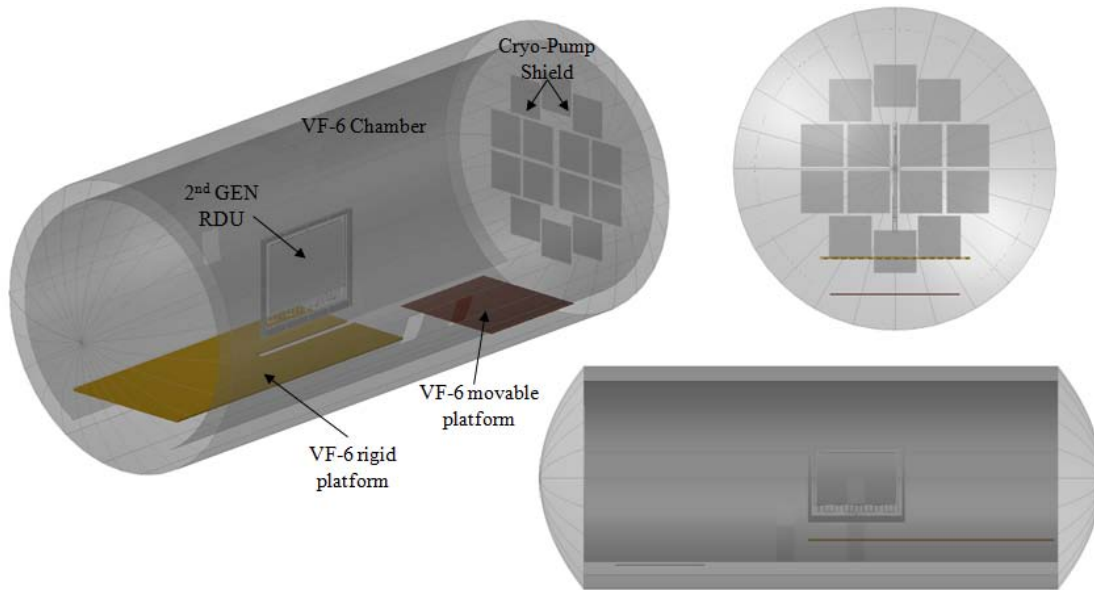
FIGURE 11. Thermal Desktop Model Of Vacuum Facility #6

The Second Generation RDU model was broken down into nodes, contactors and conductors for the analysis. VF #6 was broken down into surfaces and nodes. A total of 473 solids, 18 surfaces, 9880 nodes, 350 contactors and 1137 conductors were used in the combined model. Each surface, node, contactor and conductor was assigned a set of properties based upon the material of construction.

TABLE 1. Material Properties Used For Second Generation RDU Thermal Desktop Model

	Material	**Conductivity (W/m-K)**	**Absorptivity**	**Emissivity**
Heat Pipes & Heat Exchanger	Titanium	$K_x = K_y = K_z = 15.6$	0.52^7	0.12^7
Saddle	POCO HTC	$K_x = K_y = 70$ $K_z = 245$	NA	NA
Face sheet	K13D ($\pm 11^\circ$)	$K_x = 379$ $K_y = 14.7$ $K_z = 1.65$	0.2	0.89
Adhesive	MII Adhesive	$K_x = K_y = K_z = 8.0$	NA	NA

There are three parameters that play a significant role in the thermal analysis but are not calculated automatically within Thermal Desktop. These parameters have to be calculated outside the code and supplied as user-specified inputs to the program. The first parameter was the water to heat pipe outer wall heat transfer coefficient. The heat transfer coefficient from the coolant fluid to the heat pipe outer wall would be very difficult to calculate given the

complex geometry of annular flow around the evaporator combined with the two 90 degree bends at the entrance and exit of the heat exchanger. Instead, the flow was modeled as flow between simple concentric cylinders in order to estimate the heat transfer coefficients[8]. The heat transfer coefficients were calculated as a function of inlet water temperature. The results showed an approximately 20% reduction in heat transfer coefficient as the coolant fluid temperature decreased from 430 K to 370 K.

The internal heat pipe heat transfer coefficients in the evaporator and the condenser also could not be modeled within Thermal Desktop. For the purpose of this analysis, these coefficients were determined empirically based upon the test data. The heat transfer coefficients were calculated by iterating the heat transfer coefficient values until the average radiator surface temperature and the heat pipe outer wall temperature matched the test results within 2%. A 45% reduction in the heat transfer coefficients was observed between the highest and lowest panel temperatures.

The results from a run which did not have any heat supplied to the Second Generation RDU were used to validate the interaction between the Second Generation RDU and VF #6. The test also confirms the sink temperature calculated by Thermal Desktop. Since the radiator was receiving no heat, the average surface temperature will tend asymptotically towards the sink temperature and, with sufficient time, reach the sink temperature. The calculated average panel temperature was 151.9 K at the time when the test was terminated at about 48 hours. The measured average panel temperature was 151.4 K. The average heat sink temperature was calculated to be 150.6 K. The average sink temperature as measured by witness thermocouples attached to the side of the frame was 150.2 K. The excellent agreement between the predicted and actual values demonstrated that the model was accurately modeling the interactions and the sink temperature.

A subset of 16 tests from the 110 test runs conducted was modeled in Thermal Desktop. The tests are representative of the range of inlet water temperatures, sink temperatures and operational manifolds for full water mass flow rates (0.50 kg/s for both manifolds operating and 0.25 kg/s for one manifold operating). Given the consistency and repeatability of the test data, it was decided that successfully modeling this subset would demonstrate that the model was valid and could be used in future efforts such as the Technology Demonstration Unit where similar radiators will be used.

Analysis of the data indicated that the top row of thermocouples was not producing data that was consistent with the data for other thermocouples and RTDs during that same run. Based upon IR camera observations, this likely reflects varying amounts of NCG in the heat pipes and hence active condenser lengths. Since Thermal Desktop could not account for this and because the area involved was so small, it was decided to ignore the data from the top row of thermocouples for purposes of the model validation. This idealized the heat pipes to having little or no NCG which is likely closer to what future heat pipes will be. The small error introduced was recognized and accepted.

The actual and predicted average face sheet surface temperature for each of the 16 runs were calculated and compared. The results are shown in Table 2. The difference between the actual average panel temperature and the predicted average panel temperature was generally much less than ±1% and never exceeded ±1%. The results clearly indicate excellent agreement between the model and the test data, indicating that the model can accurately predict the face sheet temperature.

SUMMARY AND CONCLUSIONS

A radiator assembly suitable for use in a fission power system for the Moon and other applications was constructed by material innovations inc. and tested by NASA Glenn Research Center. The radiator exceeded the performance goal of dissipating 6 kW$_t$ to a 250 K sink with an inlet water temperature of 400 K and a total water mass flow rate of 0.5 kg/s by 4.6%. Models developed at NASA GRC for the Second Generation RDU showed excellent agreement with the experimental data.

Based upon these results, it was concluded that a lightweight radiator assembly could be successfully manufactured from polymer matrix composites and titanium water heat pipes and manifolds. Testing of the radiator assembly confirmed that it was capable of meeting the design goals. The testing also validated the models developed for the Second Generation RDU. The models and manufacturing experience can be used in the future for similar radiators

such as those planned for NASA GRC's Technology Demonstration Unit and for modeling more complex heat rejection systems.

TABLE 2. Comparison Of Actual And Predicted Average Panel Temperatures And Heat Rejections

Cold Wall	Operating Manifolds	Total Water Mass Flow Rate (kg/s)	Inlet Water Temperature (K)	Actual Average Panel Temperature (K)	Predicted Average Panel Temperature (K)	Panel Temperature Difference
Off	1+2	0.5	370	346.8	349.7	-0.82%
Off	1+2	0.5	400	371.9	372.5	-0.16%
Off	1+2	0.5	430	393.8	393.1	0.17%
On	1	0.25	370	313	312.3	0.21%
On	2	0.25	370	312.7	312.5	0.07%
On	1	0.25	400	334.1	335.2	-0.35%
On	2	0.25	400	337.1	334.3	0.82%
On	1	0.25	430	352.8	353.4	-0.17%
On	2	0.25	430	356.2	352.7	1.00%
On	1+2	0.5	370	335.4	336.1	-0.20%
On	1+2	0.5	380	344.6	344.8	-0.07%
On	1+2	0.5	390	352.4	352.9	-0.14%
On	1+2	0.5	400	360.6	361	-0.12%
On	1+2	0.5	410	368.3	368.4	-0.04%
On	1+2	0.5	420	376.7	376.4	0.08%
On	1+2	0.5	430	382.6	382.6	0.00%

NOMENCLATURE

A	=	area of face sheets (m²)
h	=	enthalpy of water (kJ/kg)
k	=	fin thermal conductivity (W/mK)
L	=	heat pipe spacing divided by 2 (m)
$\dot{m}$	=	mass flow (kg/s)
P_{Inlet}	=	manifold inlet water pressure (atm)
P_{Outlet}	=	manifold outlet water pressure (atm)
Q	=	heat rejected (W)
t	=	fin thickness
T_{Inlet}	=	water temperature at the manifold inlet (K)
T_{Outlet}	=	water temperature at the manifold outlet (K)
T_{Panel}	=	average radiator face sheet temperature (K)
T_{Sink} , T_S =		average sink temperature (K)
T_B	=	average fin root temperature (K)
ε	=	emissivity
ε_1	=	emissivity of front of radiator panel
ε_2	=	emissivity of back of radiator panel
η_e	=	fin efficiency
σ	=	Stefan-Boltzmann constant (5.6703 x 10^{-8} W/m²K⁴)

ACKNOWLEDGEMENTS

REFERENCES

1. Mason, L., Poston, D., and Qualls, L., "System Concepts for Affordable Fission Surface Power," NASA/TM—2008-215166, NASA, Jan. 2008.
2. Calder, J.C., "Full-scale Radiator Demonstration Unit Second Generation RDU Research & Development," NASA CR, 2010 (to be published).
3. Ellis. D.L. and Mason, L.S.. "Performance Testing Of A Full-Scale Radiator For Fission Surface Power Applications." Proc. Of 8th Annual International Energy Conversion Engineering Conference, Nashville, TN, 25 - 28 Jul 2010.
4. Gilmore, D.G., "Radiators," *Satellite Thermal Control Handbook*, edited by D.G. Gilmore and M. Bello, Aerospace Corp., El Segundo, CA. 1994, pp. 4-123 to 4-138.
5. Chang, H.V, "Optimization of a Heat Pipe Radiator Design," AIAA-84-1718, American Institute of Aeronautics and Astronautics, Reston, VA, June 1984.
6. Ellis, D.L., "Second Generation Radiator Demonstration Unit Performance Testing," NASA TM, (to be published).
7. NASA Engineering Network, Passive Thermal Control and Protection, Passive Thermal Downloads, NESC Thermal Desktop Materials List V1, URL: https://nen.nasa.gov/web/pt/downloads, May 13, 2010. Accessed January 10, 2011.
8. J.P. Holman, **Heat Transfer, Fifth Ed.**, McGraw Hill, New York, NY (1981), p. 226.